



# High quality imaging and dosimetry for yttrium-90 ( $^{90}\text{Y}$ ) liver radioembolization using a SiPM-based PET/CT scanner

Heying Duan<sup>1</sup> · Mohamed H. Khalaf<sup>2</sup> · Valentina Ferri<sup>1</sup> · Lucia Baratto<sup>1</sup> · Shyam M. Srinivas<sup>3</sup> · Daniel Y. Sze<sup>2</sup> · Andrei Iagaru<sup>1</sup>

Received: 8 October 2020 / Accepted: 2 January 2021 / Published online: 14 January 2021  
© The Author(s), under exclusive licence to Springer-Verlag GmbH, DE part of Springer Nature 2021

## Abstract

**Purpose** Transarterial radioembolization (TARE) with yttrium-90 ( $^{90}\text{Y}$ ) microspheres is a liver-directed treatment for primary and secondary hepatic malignancies. Personalized dosimetry aims for maximum treatment effect and reduced toxicity. We aimed to compare pre-treatment voxel-based dosimetry from  $^{99\text{m}}\text{Tc}$  macroaggregated albumin (MAA) SPECT/CT with post-treatment  $^{90}\text{Y}$  PET/CT for absorbed dose values, and to evaluate image quality of  $^{90}\text{Y}$  SiPM-based PET/CT.

**Methods** Forty-two patients (28 men, 14 women, mean age:  $67 \pm 11$  years) with advanced hepatic malignancies were prospectively enrolled. Twenty patients were treated with glass and 22 with resin microspheres. Radiation absorbed doses from planning  $^{99\text{m}}\text{Tc}$ -MAA SPECT/CT and post-therapy  $^{90}\text{Y}$  PET/CT were assessed.  $^{90}\text{Y}$  PET/CT images were acquired for 20 min and reconstructed to produce 5-, 10-, 15-, and 20-min datasets, then evaluated using the 5-point Likert scale.

**Results** The mean administered activity was  $3.44 \pm 1.5$  GBq for glass and  $1.62 \pm 0.7$  GBq for resin microspheres. The mean tumor absorbed doses calculated from  $^{99\text{m}}\text{Tc}$ -MAA SPECT/CT and  $^{90}\text{Y}$  PET/CT were  $175.69 \pm 113.76$  Gy and  $193.58 \pm 111.09$  Gy ( $P = 0.61$ ), respectively for glass microspheres; they were  $60.18 \pm 42.20$  Gy and  $70.98 \pm 49.65$  Gy ( $P = 0.37$ ), respectively for resin microspheres. The mean normal liver absorbed doses from  $^{99\text{m}}\text{Tc}$ -MAA SPECT/CT and  $^{90}\text{Y}$  PET/CT were  $32.70 \pm 22.25$  Gy and  $30.62 \pm 20.09$  Gy ( $P = 0.77$ ), respectively for glass microspheres; they were  $18.33 \pm 11.08$  Gy and  $24.32 \pm 15.58$  Gy ( $P = 0.17$ ), respectively for resin microspheres. Image quality of  $^{90}\text{Y}$  PET/CT at 5-, 10-, 15-, and 20-min scan time showed a Likert score of  $3.6 \pm 0.54$ ,  $4.57 \pm 0.58$ ,  $4.84 \pm 0.37$ , and  $4.9 \pm 0.3$ , respectively.

**Conclusions**  $^{99\text{m}}\text{Tc}$ -MAA SPECT/CT demonstrated great accuracy for treatment planning dosimetry. SiPM-based PET/CT scanner showed good image quality at 10-min scan time, acquired in one bed position. A PET/CT scan time of 5 min showed acceptable image quality and suffices for dosimetry and treatment verification. This allows for inclusion of  $^{90}\text{Y}$  PET/CT in busy routine clinical workflows. Studies with larger patient cohorts are needed to confirm these findings.

**Keywords**  $^{90}\text{Y}$  · Silicon photomultiplier · PET/CT · Radioembolization · SIRT · Liver · Dosimetry

This article is part of the Topical Collection on Dosimetry

✉ Andrei Iagaru  
aiagaru@stanford.edu

Heying Duan  
heying@stanford.edu

<sup>1</sup> Department of Radiology, Division of Nuclear Medicine and Molecular Imaging, Stanford University, 300 Pasteur Drive, H2200, Stanford, CA 94305, USA

<sup>2</sup> Department of Radiology, Division of Interventional Radiology, Stanford University, Stanford, CA, USA

<sup>3</sup> Department of Radiology, Division of Nuclear Medicine, University of Pittsburgh Medical Center, Pittsburgh, PA, USA

## Introduction

Transarterial radioembolization (TARE) is now an established minimally invasive liver-directed treatment modality. It is used to treat unresectable primary liver cancer, like hepatocellular carcinoma (HCC) and intrahepatic cholangiocarcinoma (ICC), or hepatic metastases from other tumors [1]. Currently, two types of microspheres are available for clinical use: glass (TheraSphere®; Boston Scientific, Marlborough, MA, USA) and resin (SIR-Spheres®; Sirtex, Boston, MA, USA). Several studies have shown that TARE extends progression-free and overall survival [2–5]. However, treatment efficacy is correlated to tumor absorbed dose and toxicity is determined by the dose to the surrounding, healthy liver tissue [6, 7].

**Table 1** Patient characteristics (*n* = 42)

All patients		
Gender	28 males, 14 females	
Age (years)	67 ± 11.5 (range: 40 – 88)	
Primary hepatic cancer	<i>n</i> = 27 (64.3%)	
HCC	18 (42.9 %)	
ICC	8 (19 %)	
Mixed HCC/ICC	1 (2.4 %)	
Hepatic metastases	<i>n</i> = 15 (35.7%)	
Colorectal carcinoma	9 (21.4 %)	
Leiomyosarcoma	3 (7.1 %)	
Melanoma	2 (4.8 %)	
Pancreatic carcinoma	1 (2.4 %)	
Patients divided by type of microsphere used		
	Glass microspheres	Resin microspheres
Total	20	22
Primary hepatic cancer	19	8
Hepatic metastases	1	14
Administered activity (GBq)	3.44 ± 1.5 (range 0.93–7.05)	1.62 ± 0.7 (range 0.56–3.15)

HCC hepatocellular carcinoma, ICC intrahepatic cholangiocarcinoma

Personalized dosimetry is therefore paramount to keep toxicity at a minimum while aiming for maximal treatment effect. Depending on glass or resin microspheres, different activity calculation models apply. However, the radiation absorbed doses in the tumor(s) vs. the normal liver tissue are not determined [8, 9].

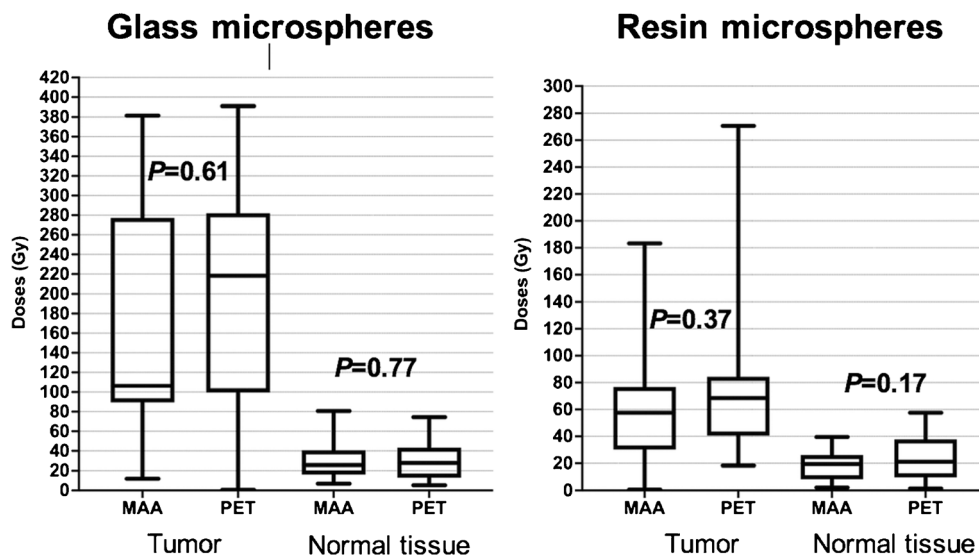
Treatment planning consists of a TARE simulation with an injection of Technetium-99 m (<sup>99m</sup>Tc)-labeled macroaggregated albumin (MAA) in the location(s) of planned <sup>90</sup>Y-microsphere delivery, and planar and single-photon emission computed tomography/computed tomography (SPECT/CT) imaging to quantify the lung-shunt fraction (LSF) and to evaluate for collateral extrahepatic tracer deposition. MAA mimics <sup>90</sup>Y-microsphere distribution but due to differences in size, shape, and number of particles, it can only give an estimate for radiation absorbed doses for dosimetry [10–14]. Imaging for treatment verification can be performed with <sup>90</sup>Y bremsstrahlung SPECT/CT

[15]. However, acquisition time is long, and image quality is low [16]. The decay of <sup>90</sup>Y produces a positron and electron pair every 32 in 1 million decays allowing for imaging with PET [17]. Despite the higher resolution, image acquisition time is still long, and image quality is sub-optimal [18]. Recent technical advances in PET/CT scanners resulted in the development of detectors which combine lutetium-based scintillator crystal arrays with a silicon photomultiplier (SiPM) bloc design leading to higher spatial resolution and with improved reconstruction algorithms, enhance image quality. Not only did hardware advance, currently there are different types of software available to facilitate dosimetry. Several studies indicate that the 3-dimensional voxel-based dosimetry is most accurate in prediction of activity distribution [19–21]. However, clinical studies assessing concordance of 3-dimensional voxel-based dosimetry comparing <sup>99m</sup>Tc-MAA SPECT/CT and post-treatment <sup>90</sup>Y PET/CT are lacking.

**Table 2** Radiation absorbed doses of simulation <sup>99m</sup>Tc MAA SPECT/CT and post-treatment <sup>90</sup>Y PET/CT, divided per used microsphere type

	Glass microspheres		Resin microspheres	
	<sup>99m</sup> Tc MAA SPECT/CT	<sup>90</sup> Y PET/CT	<sup>99m</sup> Tc MAA SPECT/CT	<sup>90</sup> Y PET/CT
Tumor dose (Gy)	175.69 ± 113.76 (range 11.91–381.41) <i>P</i> = 0.61	193.58 ± 111.09 (range 0.68–391.07)	60.18 ± 42.20 (range 0.71–183.25) <i>P</i> = 0.37	70.98 ± 49.65 (range 18.32–270.64)
Normal liver tissue dose (Gy)	32.70 ± 22.25 (range 6.93–80.68) <i>P</i> = 0.77	30.62 ± 20.09 (range 5.29–74.43)	18.33 ± 11.08 (range 2.21–39.50) <i>P</i> = 0.17	24.32 ± 15.81 (range 1.45–57.61)

**Fig. 1** Boxplot visualization of radiation absorbed doses of pre-treatment <sup>99m</sup>Tc-MAA SPECT/CT and post-treatment <sup>90</sup>Y PET/CT for glass and resin microspheres



In this study, we performed personalized, voxel-based dosimetry for radiation absorbed doses based on planning <sup>99m</sup>Tc-MAA SPECT/CT and post-treatment <sup>90</sup>Y PET/CT and evaluated the image quality of SiPM-based PET/CT after <sup>90</sup>Y radioembolization.

**Material and methods**

**Participants**

We prospectively enrolled consecutive patients with unresectable primary or secondary hepatic malignancies who were scheduled for TARE at our institution. All patients had a diagnostic CT or MRI prior to TARE planning. The administered activity was calculated using the respective vendor’s recommendation: the body surface area (BSA) method was used for resin microspheres and the partition model for glass microspheres. Written informed consent was obtained from all included patients. This study has been approved by the local

institutional review board and was registered on [clinicaltrials.gov](https://clinicaltrials.gov) (NCT03109262).

**Pre-treatment <sup>99m</sup>Tc-MAA SPECT/CT protocol**

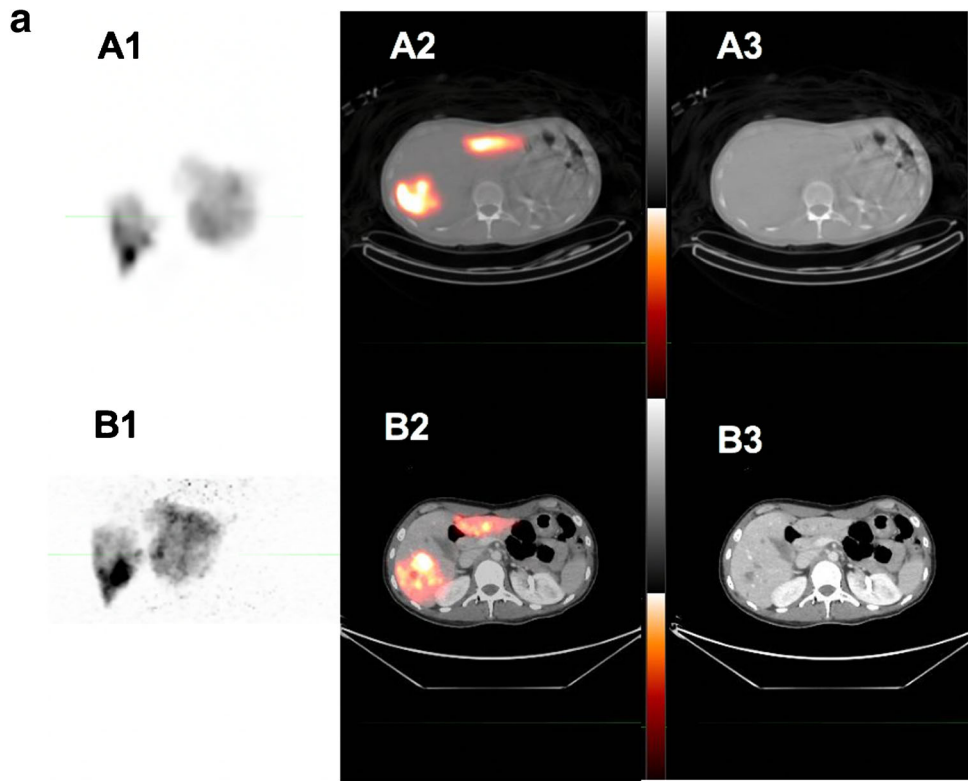
Patients had <sup>99m</sup>Tc-MAA imaging as part of the standard TARE planning protocol. The intraarterial administration of 148 MBq <sup>99m</sup>Tc-MAA in the Interventional Radiology suite was followed by anterior and posterior whole-body planar imaging in Nuclear Medicine to quantify LSF. Then a SPECT/CT of the upper abdomen was performed using a dual detector gamma-camera (Infinia Hawkeye 4, Discovery 670 DR or Discovery 870 CZT, GE Healthcare, Waukesha, WI, USA). Images were reconstructed using ordered subset expectation maximization (OSEM).

**Post-treatment <sup>90</sup>Y SiPM PET/CT protocol**

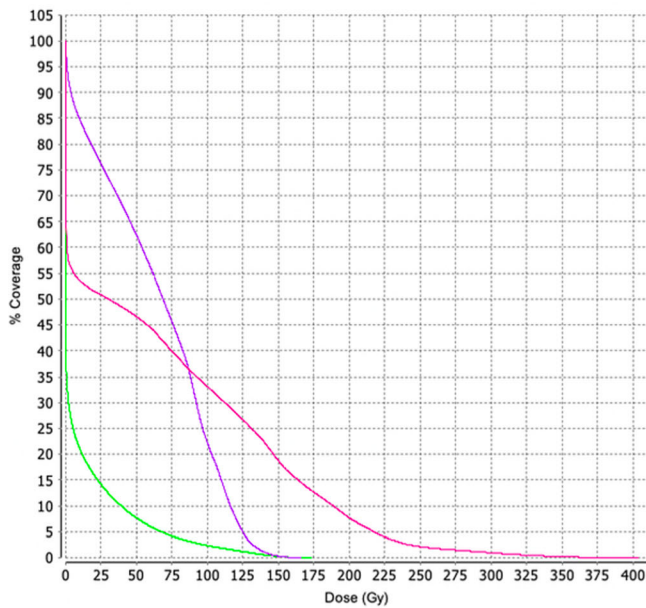
Images were acquired within 24 h after TARE using a SiPM-based PET/CT (Discovery MI, GE Healthcare). A

**Table 3** Radiation absorbed doses from planning <sup>99m</sup>Tc-MAA SPECT/CT and post-treatment <sup>90</sup>Y PET/CT when catheter tip position was changed at TARE, per used microsphere type

	Glass microspheres		Resin microspheres	
	<sup>99m</sup> Tc-MAA SPECT/CT	<sup>90</sup> Y PET/CT	<sup>99m</sup> Tc-MAA SPECT/CT	<sup>90</sup> Y PET/CT
Tumor dose (Gy)	155.11 ± 107.83 (range: 11.91–353.10) <i>P</i> = 0.35	203.21 ± 105.78 (range: 0.68–344.44)	62.32 ± 44.59 (range: 0.71–160.78) <i>P</i> = 0.98	61.97 ± 32.22 (range: 20.75–130.03)
Normal liver dose (Gy)	39.23 ± 27.62 (range: 12.28–80.68) <i>P</i> = 0.57	30.50 ± 27.95 (range: 5.67–74.43)	22.26 ± 10.83 (range: 3.46–33.75) <i>P</i> = 0.14	33.48 ± 17.03 (range: 8.83–57.61)

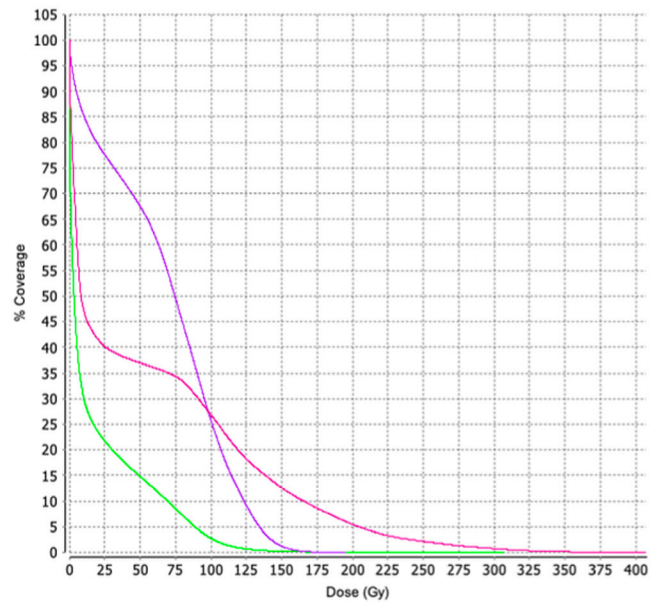


**b** Planning <sup>99m</sup>Tc-MAA SPECT/CT



Dose ID	Dose Details				
D1	LDM with Known Activity Dose				
Contour	Line Style	Max Dose	Min Dose	Mean Dose	SD
Normal Tissue	D1	D1	D1	D1	D1
Normal Tissue	—	174.37	0.00	10.84	25.37
Tumor 1	—	410.37	0.00	68.54	80.33
Tumor 2	—	167.92	0.00	64.45	40.78

Post-treatment <sup>90</sup>Y PET/CT



Dose ID	Dose Details				
D1	LDM with Known Activity Dose				
Contour	Line Style	Max Dose	Min Dose	Mean Dose	SD
Normal Tissue	D1	D1	D1	D1	D1
Normal Tissue	—	307.03	0.00	17.63	30.07
Tumor 1	—	407.29	0.00	55.53	73.65
Tumor 2	—	194.53	0.00	69.04	42.43

**Fig. 2** Forty-six-year-old woman patient with new hepatic metastases in liver segment 6 and in the left lobe originating from sigmoid adenocarcinoma. **a** Pre-treatment planning with SPECT/CT (A1, maximum intensity projection, MIP; A2–A3, axial fused SPECT/CT, and CT, respectively) after intraarterial delivery of 163 MBq  $^{99m}\text{Tc}$ -MAA via the segment 6 artery and segment 2/3 trunk. Hepato-pulmonary shunt was 1.4%. Post-treatment SiPM PET/CT (B1, MIP; B2–B3, axial fused PET/CT, and CT, respectively) obtained after administration of 0.47 GBq  $^{90}\text{Y}$ -resin spheres via the segment 6 artery and 0.45 GBq via the segment 2/3 trunk.  $^{90}\text{Y}$  PET/CT shows true distribution of microspheres with no extrahepatic uptake. **b** Dose-volume histogram of simulation  $^{99m}\text{Tc}$ -MAA SPECT/CT and  $^{90}\text{Y}$  PET/CT

diagnostic contrast-enhanced CT of the upper abdomen was obtained after the administration of 50 mL iodinated contrast media using 120 kV, “smart” modulating mA and a  $512 \times 512$  matrix size. Thereafter, a PET scan was acquired in 3D mode using a single bed position located over the liver, with a total acquisition time of 20 min. The DMI scanner at our institution has an axial field of view of 20 cm. Each field of view contains 71 slices (2.79 mm). The PET emission scan was corrected using the segmented attenuation data of the CT scan and reconstructed both with a standard iterative algorithm (OSEM, 2 iterations, 28 subsets), as well as the vendor recommended reconstruction method, the block sequential regularized expectation maximization (BSREM) (Q.Clear; GE Healthcare).  $^{90}\text{Y}$  PET/CT scans were reconstructed as 5-, 10-, 15-, and 20-min datasets to determine image quality at these scan times.

Catheter position of  $^{99m}\text{Tc}$ -MAA and  $^{90}\text{Y}$ -microsphere injection was documented and intended treatment approach, e.g., whole liver vs. lobar vs. segmental.

### Image analysis

All images were reformatted into axial, coronal, and sagittal views.

$^{99m}\text{Tc}$ -MAA planning SPECT/CT was compared to  $^{90}\text{Y}$  PET/CT to assess the accuracy of tracer/microsphere distribution. Three-dimensional voxel-based dosimetry was performed using the MIM SurePlan™ software (MIM Software version 6.9.2., Cleveland, OH, USA). This software converts counts per voxel to radiation absorbed dose measured in Gray (Gy). Whole liver and tumor(s) were edge-contoured on the diagnostic CT or MRI obtained prior to TARE planning. These contours were then transferred to  $^{99m}\text{Tc}$ -MAA SPECT/CT and  $^{90}\text{Y}$  PET/CT images using deformable registration to calculate estimated normal liver tissue and tumor radiation absorbed dose, and to assess post-treatment absorbed doses, respectively.

Image quality of SiPM-based PET/CT was evaluated using the 5-point Likert scale (1 non-diagnostic, 2 suboptimal image quality, 3 acceptable image quality, 4 good image quality, 5

excellent image quality). Images were reviewed and analyzed independently in random order by two experienced Nuclear Medicine physicians.

### Statistical analysis

Statistical analysis was performed with Prism GraphPad v8.3.0 (GraphPad Software, San Diego, CA, USA).

A two-tailed paired student's *t* test was performed to determine differences between  $^{99m}\text{Tc}$ -MAA SPECT/CT and  $^{90}\text{Y}$  PET/CT. A *P* value of  $< 0.05$  was considered statistically significant. Continuous data are presented as mean  $\pm$  standard deviation (SD), range: minimum (min)–maximum (max) values.

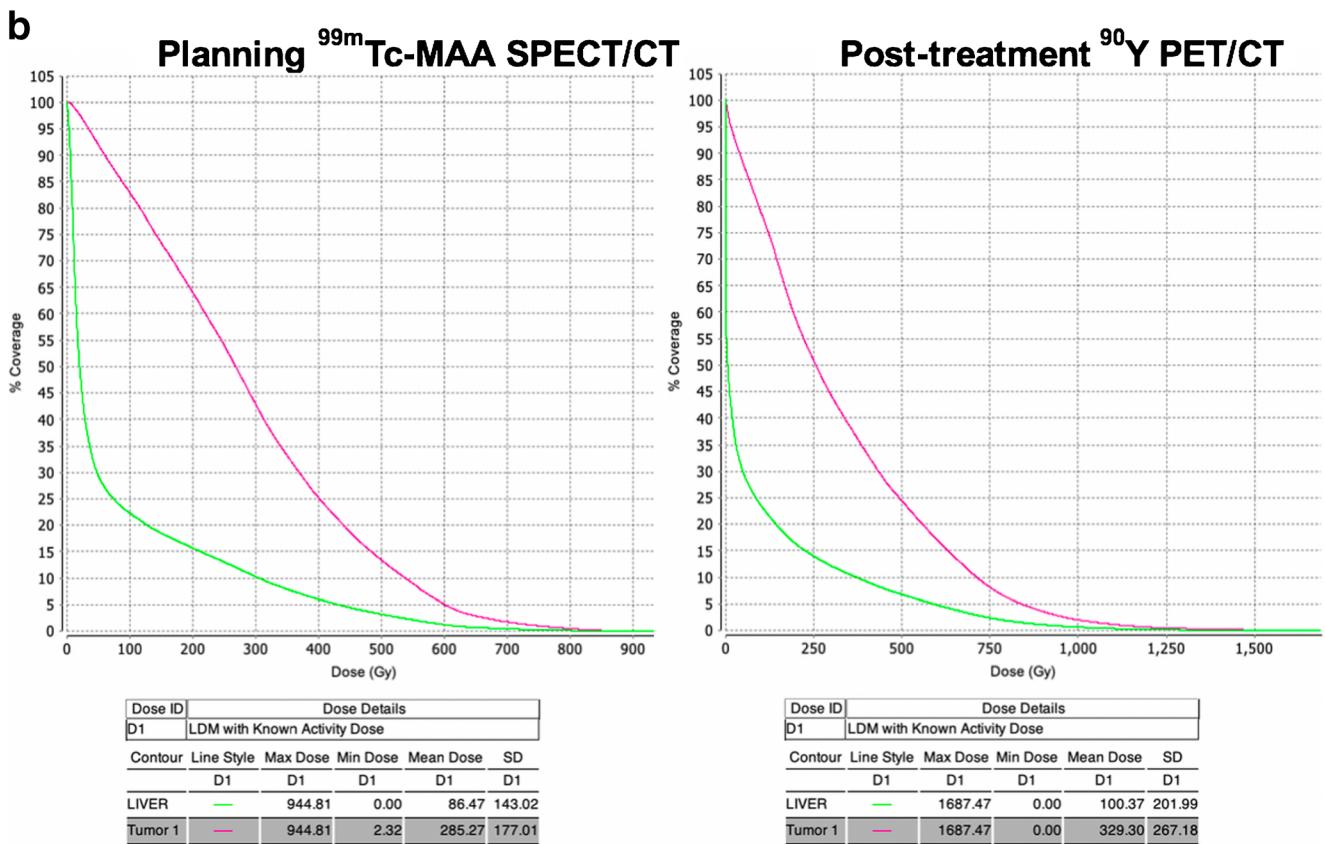
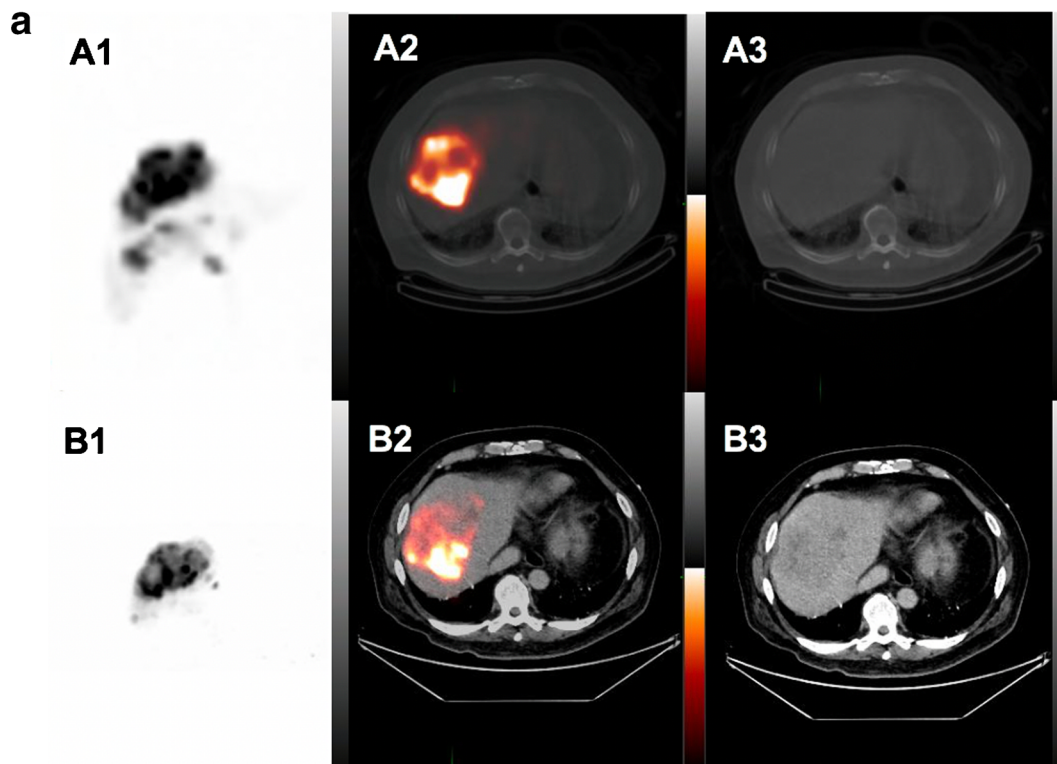
### Results

Forty-two patients (28 males, 14 females, mean age  $67 \pm 11$  (range: 40–88) years) with unresectable, advanced hepatic malignant lesions were prospectively enrolled in this study. The patients were divided into two groups according to the type of microspheres used: 20 patients received TARE with glass and 22 with resin microspheres. The mean administered activity for  $^{90}\text{Y}$  glass microspheres was  $3.44 \pm 1.5$  (range: 0.93–7.05) GBq and  $1.62 \pm 0.7$  (range: 0.56–3.15) GBq for  $^{90}\text{Y}$  resin. Patients' characteristics are shown in Table 1.

### Comparison of dosimetry estimated from $^{99m}\text{Tc}$ -MAA SPECT/CT and $^{90}\text{Y}$ PET/CT

The mean tumor absorbed dose estimated from  $^{99m}\text{Tc}$ -MAA SPECT/CT was  $175.69 \pm 113.76$  (range: 11.91–381.41) Gy vs.  $193.58 \pm 111.09$  (range: 0.68–391.07) Gy from  $^{90}\text{Y}$  PET/CT for glass microspheres and  $60.18 \pm 42.20$  (range: 0.71–183.25) Gy vs.  $70.98 \pm 49.65$  (range: 18.32–270.64) Gy respectively for resin microspheres. For normal liver, the mean absorbed dose from  $^{99m}\text{Tc}$ -MAA, SPECT/CT was  $32.70 \pm 22.25$  (range: 6.93–80.68) Gy, and  $30.62 \pm 20.09$  (range: 5.29–74.43) Gy from  $^{90}\text{Y}$  PET/CT for glass microspheres, and  $18.33 \pm 11.08$  (range: 2.21–39.50) Gy and  $24.32 \pm 15.81$  (range: 1.45–57.61) Gy for resin, respectively. Radiation absorbed doses for tumors and normal liver tissue were not significantly different between  $^{99m}\text{Tc}$ -MAA SPECT/CT and  $^{90}\text{Y}$  PET/CT neither for glass ( $P = 0.61$  and  $P = 0.77$ ) nor resin ( $P = 0.37$  and  $P = 0.17$ ) microspheres, indicating high concordance of  $^{99m}\text{Tc}$ -MAA SPECT/CT and  $^{90}\text{Y}$  PET/CT and predictive accuracy of  $^{99m}\text{Tc}$ -MAA SPECT/CT for absorbed doses for tumor and healthy liver tissue. Data are shown in Table 2 and Fig. 1.

In 24 patients (57.1%),  $^{90}\text{Y}$ -microspheres were administered in the same location as  $^{99m}\text{Tc}$ -MAA in the planning



angiography and showed great accuracy in distribution (Fig. 2). In 18 patients (42.9%), <sup>90</sup>Y-microspheres were injected

differently, either more selectively or only to one lobe for a sequential treatment approach. For glass microspheres (*n* = 8),

**Fig. 3** Sixty-five-year-old male patient with a large HCC in segment 8/7 measuring 10.4 × 8.8 × 7.5 cm. He was treated with glass microspheres in a palliative attempt to control the growth of disease and cause hypertrophy in the left lobe in preparation for surgery. **a** Pre-treatment planning with SPECT/CT (A1, MIP; A2-A3, axial fused SPECT/CT, and CT, respectively) after intraarterial delivery of 111 MBq <sup>99m</sup>Tc-MAA via the right and 48 MBq via the left hepatic artery. Hepato-pulmonary shunt was 3%. Post-treatment SiPM PET/CT (B1, MIP; B2-B3, axial fused PET/CT, and CT, respectively) obtained after selective administration of 0.81 GBq <sup>90</sup>Y-glass microspheres via the segment 7, 2.73 GBq via the segment 5/8 trunk and 0.95 GBq via the segment 4 artery. <sup>90</sup>Y PET/CT shows selective distribution of microspheres in the tumor. **b** Dose-volume histogram of simulation <sup>99m</sup>Tc-MAA SPECT/CT and <sup>90</sup>Y PET/CT

we observed a non-significant upward trend in tumor absorbed dose with 203.21 ± 105.78 (range: 0.68–344.44) Gy calculated from <sup>90</sup>Y PET/CT vs. 155.11 ± 107.83 (range: 11.91–353.10) Gy from <sup>99m</sup>Tc-MAA SPECT/CT (*P* = 0.35). This trend was not seen in normal tissue absorbed dose which stayed consistent with 39.23 ± 27.62 (range: 12.28–80.68) Gy from <sup>99m</sup>Tc-MAA SPECT/CT vs. 30.50 ± 27.95 (range: 5.67–74.43) Gy calculated from <sup>90</sup>Y PET/CT (*P* = 0.57). Figure 3 shows a patient treated with glass microspheres with a sequential treatment approach and selective treatment of liver segment 1. For resin microspheres (*n* = 10), different catheter position did not make a change in absorbed doses: For tumor, 62.32 ± 44.59 (range: 0.71–160.78) Gy calculated from <sup>99m</sup>Tc-MAA SPECT/CT vs. 61.97 ± 32.22 (range: 20.75–130.03) Gy from <sup>90</sup>Y PET/CT (*P* = 0.98); and for normal liver tissue, 22.26 ± 10.83 (range: 3.46–33.75) Gy vs. 33.48 ± 17.03 (range: 8.83–57.61) Gy (*P* = 0.14), respectively. Data are shown in Table 3.

2A total of 21 patients (50%) were treated for a single tumor and another 21 patients (50%) for multiple liver

**Table 5** Image quality of SiPM-based <sup>90</sup>Y-PET/CT

Scan time	<sup>90</sup> Y PET/CT
5 min	3.6 ± 0.54 (range 3–4)
10 min	4.57 ± 0.58 (range 3–5)
15 min	4.8 ± 0.37 (range 4–5)
20 min	4.9 ± 0.3 (range 4–5)

*P* value of < 0.05 was considered statistically significant

tumors. Tumor absorbed doses for single tumor treatment were 126.11 ± 90.24 (range: 29.23–347.64) Gy vs. 144.66 ± 93 (range: 20.75–344.44) Gy from <sup>99m</sup>Tc-MAA SPECT/CT and <sup>90</sup>Y PET/CT respectively (*P* = 0.52). For multiple tumors, absorbed doses were slightly lower with 99.84 ± 89.23 (range: 0.71–353.1) Gy from <sup>99m</sup>Tc-MAA SPECT/CT vs. 109.01 ± 91.73 (range: 5.26–326.98) Gy from <sup>90</sup>Y PET/CT respectively (*P* = 0.69). When tumor absorbed doses from <sup>99m</sup>Tc-MAA SPECT/CT and <sup>90</sup>Y PET/CT for single tumor and multiple tumor treatment were compared to each other, no significant difference was seen (*P* = 0.31 vs. *P* = 0.18). No statistically significant difference was seen in normal liver tissue as well. Data are shown in Table 4.

**Image quality of SiPM-based PET/CT**

The best image quality was seen at a scan time of 20 min with a Likert score of 4.9 ± 0.3 (range: 4–5). There was no significant difference between a scan time of 20 min and 15 min (4.84 ± 0.37, range: 4–5, *P* = 0.3). Image quality improved significantly from 5 min (3.6 ± 0.54, range: 3–4) to 10 min scan time (4.57 ± 0.58, range: 3–

**Table 4** Radiation absorbed doses of planning <sup>99m</sup>Tc MAA SPECT/CT and post-treatment <sup>90</sup>Y PET/CT, divided per single versus multiple tumors treated

	Single tumor treatment		Multiple tumor treatment	
	<sup>99m</sup> Tc MAA SPECT/CT	<sup>90</sup> Y PET/CT	<sup>99m</sup> Tc MAA SPECT/CT	<sup>90</sup> Y PET/CT
Tumor dose (Gy)	126.11 ± 90.24 (range 29.23–347.64) <i>P</i> = 0.52	144.66 ± 93 (range 20.75–344.44)	99.84 ± 89.23 (range 0.71–353.10) <i>P</i> = 0.69	109.01 ± 91.73 (range 5.26–326.98)
Normal liver tissue dose (Gy)	24.42 ± 16.05 (range 5.86–74.71) <i>P</i> = 0.85	23.45 ± 16.60 (range 3.16–57.61)	26.81 ± 20.52 (range 2.21–73.55) <i>P</i> = 0.71	29.44 ± 18.61 (range 1.45–74.43)
Tumor dose <sup>99m</sup> Tc MAA SPECT/CT	Single tumor treatment <i>P</i> = 0.31		Multiple tumor treatment	
<sup>90</sup> Y PET/CT	<i>P</i> = 0.18			
Normal liver tissue dose <sup>99m</sup> Tc MAA SPECT/CT	Single tumor treatment <i>P</i> = 0.71		Multiple tumor treatment	
<sup>90</sup> Y PET/CT	<i>P</i> = 0.32			

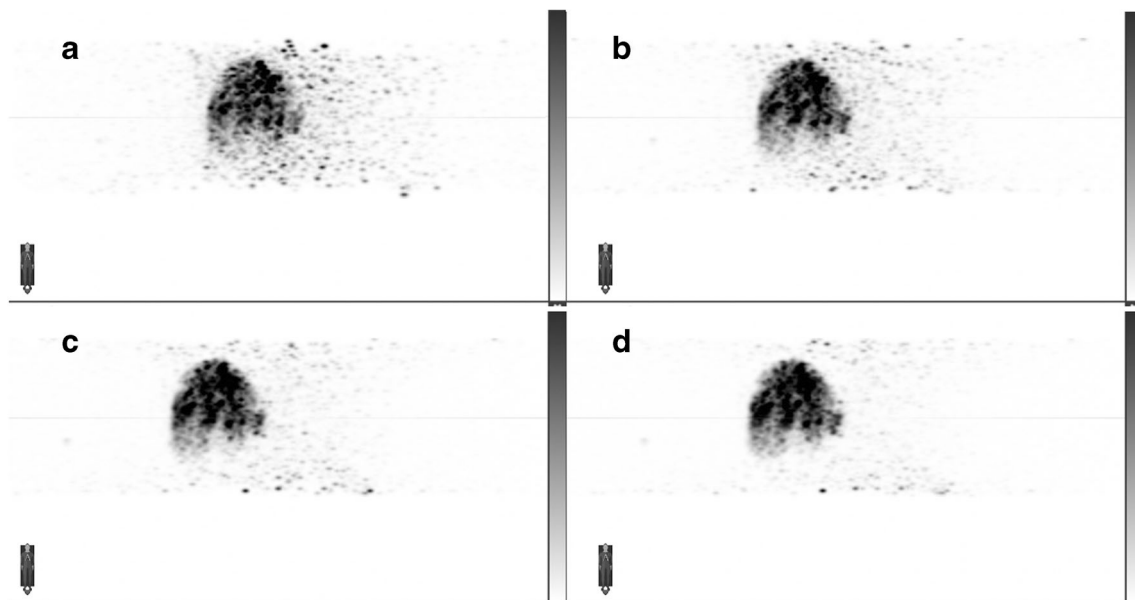


**Fig. 4** Eighty-year-old man patient with HCC. Post-treatment SiPM PET/CT after administration of 1.5 GBq  $^{90}\text{Y}$ -glass microspheres via the right hepatic artery. Images were reconstructed at different scan times:

5 min (**a**, MIP), 10 min (**b**, MIP), 15 min (**c**, MIP), and 20 min (**d**, MIP). Image **a** showed good image quality at 5 min scan time in a single bed position

5,  $P = 0.000$ ) as well as from 10 min to 15 min ( $P = 0.001$ ). Data are shown in Table 5. However, a scan time of 5 min suffices for treatment verification and dosimetry (Fig. 4).

In 3 patients,  $^{90}\text{Y}$  PET/CT was obtained 24 h after TARE. Figure 5 shows these images reconstructed with OSEM and BSREM at 10-min and 15-min scan time. Image quality was deemed excellent (Likert scale  $4.75 \pm$

0.5, range: 4–5) with both reconstruction methods; however, BSREM was superior.

## Discussion

In this prospective study, we evaluated voxel-based dosimetry data and image quality of  $^{90}\text{Y}$  PET/CT after TARE using a new generation scanner based on SiPM

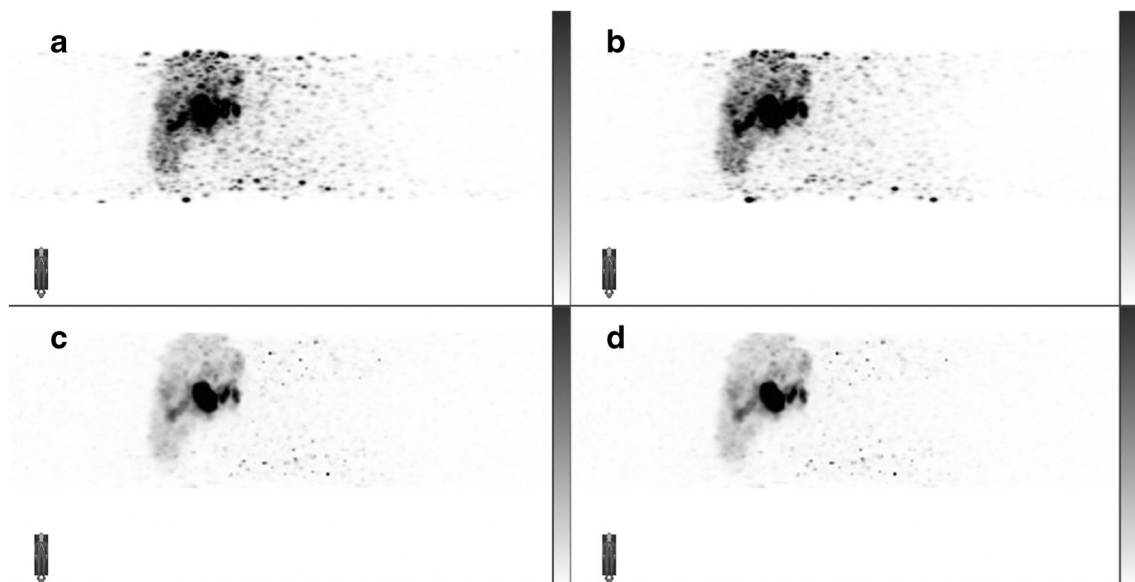


**Fig. 5** Eighty-four-year-old man patient with HCC. Post-treatment SiPM PET/CT was obtained 24 h after administration of 1.84 GBq  $^{90}\text{Y}$ -glass microspheres via the right hepatic artery. Images were reconstructed at

10 min (**a**, **c** MIP) and at 15 min scan time (**b**, **d** MIP) using OSEM (**a**, **b**) and BSREM (**c**, **d**) reconstruction algorithm. BSREM shows higher image quality



which shows a higher spatial resolution and allows for improved reconstruction methods like the BSREM algorithm, all resulting in higher sensitivity and image quality [22, 23].

Post-treatment imaging can either be performed with bremsstrahlung SPECT/CT or low-abundance internal pair production PET/CT. SPECT/CT has poor spatial resolution due to detector efficiency, leading to noisy images and long acquisition times [16]. Standard time of flight (ToF) PET provides higher image quality, but still requires a long scan time of approximately 30 min and multiple bed positions [24–26]. To date, no studies evaluating SiPM-based PET/CT for post-treatment  $^{90}\text{Y}$  imaging have been published. Kunnen et al. compared the performance of a digital PET/CT to an analog PET/CT based on photomultiplier tubes (PMT) in a phantom study to determine the best reconstruction setting for the digital PET/CT [27]. No clinically significant differences were found between the two scanner systems. Visually, the digital PET/CT showed less noise but on a quantitative level, both scanners were equal. Our data show excellent image quality of SiPM-based PET/CT at a scan time of 20 min in a single bed position. However, a short scan time of 5 min showed acceptable to good image quality and suffices for treatment verification and dosimetry calculation. Early visualization of inadvertently extrahepatic  $^{90}\text{Y}$  deposition post-therapy is important as interventions can be made accordingly in a timely manner to confine complications.

Dosimetry uses the pre-treatment planning  $^{99\text{m}}\text{Tc}$ -MAA SPECT/CT to estimate the tumor dose to ensure the delivery of a tumorcidal dose while sparing the surrounding healthy liver tissue. Since MAA is different to  $^{90}\text{Y}$ -microspheres, it can only give an estimate of tumor absorbed dose. There are multiple studies comparing estimated doses from  $^{99\text{m}}\text{Tc}$ -MAA SPECT/CT and verified doses from post-treatment imaging with controversial results. Some have shown differences [13, 28] while others found a better correlation in primary liver tumors than metastatic liver disease [28, 29]. Most studies comparing pre-treatment  $^{99\text{m}}\text{Tc}$ -MAA SPECT/CT and post-treatment  $^{90}\text{Y}$  bremsstrahlung or PET/CT use manually drawn region of interests or rigid contours over tumor and normal liver tissue to quantify for mean counts per pixel and to evaluate the tumor to background ratio [28, 30, 31]. In this study, we used 3-dimensional, voxel-based dosimetry and converted counts per voxel to radiation absorbed dose measured in Gray by taking tumor volume and total liver volume into account. We used a local deposition model with scaling for a known injected activity for simulation  $^{99\text{m}}\text{Tc}$ -MAA SPECT/CT and post-treatment  $^{90}\text{Y}$  PET/CT. Our data show that absorbed doses of the tumor and normal liver tissue from  $^{99\text{m}}\text{Tc}$ -MAA SPECT/CT were not significantly different to post-treatment  $^{90}\text{Y}$  PET/CT even when stratified for single vs. multiple tumors treated.

$^{99\text{m}}\text{Tc}$ -MAA SPECT/CT accurately predicted the absorbed dose of the tumor and normal liver tissue. This indicates a high accuracy of  $^{99\text{m}}\text{Tc}$ -MAA based dosimetry.

The catheter tip position at the administration of  $^{99\text{m}}\text{Tc}$ -MAA and  $^{90}\text{Y}$ -microspheres might contribute to discrepancies of absorbed doses [10]. Our data show that when the catheter position was changed, it was for selective lobar/segmental treatment approach which resulted in no significant difference in absorbed doses between  $^{99\text{m}}\text{Tc}$ -MAA SPECT/CT and  $^{90}\text{Y}$  PET/CT. Only in glass microspheres, a not significant trend to higher tumor absorbed dose was observed in post-treatment  $^{90}\text{Y}$  PET/CT, suggesting that a more selective treatment might lead to a higher tumor dose. However, this needs to be confirmed in larger and more homogenous patient cohorts.

Depending on which microspheres are administered, different treatment activity calculation models apply. For resin microspheres, a semiempirical method relying on the BSA is used, and for glass microspheres, a whole liver partition model is used, based on medical internal radiation dose (MIRD) principles. Both do not calculate the radiation absorbed dose in the tumors and normal liver tissue. Using accurate dosimetry methods, individualized tumor dose intensification can be made possible to maximize treatment effect while not exceeding the maximal tolerated dose of healthy liver tissue.

Limitations of this study include the small and heterogeneous patient cohort. A variety of primary and metastatic liver tumors were treated with resin microspheres whereas glass microspheres were majorly used for primary hepatic malignancies. In total, more patients (27 vs. 15) received TARE for their primary liver tumor. Since this was a very heterogeneous patient population with various types of tumor entities, we did not analyze the impact of treatment in terms of response rate and progression-free survival.

## Conclusion

$^{99\text{m}}\text{Tc}$ -MAA SPECT/CT showed great accuracy in predicting the absorbed dose of the tumor and normal liver tissue. Good image quality was seen at a reduced scan time of 10 min with SiPM-based  $^{90}\text{Y}$  PET/CT, acquired in a single bed position. A PET/CT scan time of 5 min showed acceptable image quality and suffices for dosimetry and treatment verification. A short scan time allows for the inclusion of  $^{90}\text{Y}$  PET/CT in busy routine clinical workflows. Studies with larger patient cohorts are needed to confirm these findings.

**Authors' contributions** HD: content planning, data analyses, and manuscript writing and editing; MHK: data analyses and manuscript editing; VF: statistical analyses and manuscript editing; LB: data analyses and manuscript editing; SMS: concept planning and data manuscript editing;

DYS: content planning and manuscript editing; AI content planning and manuscript editing

**Funding** The study was partially supported by GE Healthcare.

**Data availability** Yes.

## Compliance with ethical standards

**Conflict of interest** The authors declare that they have no conflict of interest.

**Ethics approval** Yes.

**Consent to participate** Yes.

**Consent for publication** Yes.

**Code availability** Yes.

## References

- Voutsinas N, Lekperic S, Barazani S, Titano JJ, Heiba SI, Kim E. Treatment of primary liver tumors and liver metastases, Part 1: Nuclear Medicine Techniques. *J Nucl Med*. 2018;59:1649–54. <https://doi.org/10.2967/jnumed.116.186346>.
- Coldwell D, Sangro B, Salem R, Wasan H, Kennedy A. Radioembolization in the treatment of unresectable liver tumors: experience across a range of primary cancers. *Am J Clin Oncol*. 2012;35:167–77. <https://doi.org/10.1097/COC.0b013e3181f47923>.
- Sangro B, Salem R, Kennedy A, Coldwell D, Wasan H. Radioembolization for hepatocellular carcinoma: a review of the evidence and treatment recommendations. *Am J Clin Oncol*. 2011;34:422–31. <https://doi.org/10.1097/COC.0b013e3181df0a50>.
- Sangro B, Carpanese L, Cianni R, Golfieri R, Gasparini D, Ezziddin S, et al. Survival after yttrium-90 resin microsphere radioembolization of hepatocellular carcinoma across Barcelona clinic liver cancer stages: a European evaluation. *Hepatology*. 2011;54:868–78. <https://doi.org/10.1002/hep.24451>.
- Seidensticker R, Denecke T, Kraus P, Seidensticker M, Mohnike K, Fahlke J, et al. Matched-pair comparison of radioembolization plus best supportive care versus best supportive care alone for chemotherapy refractory liver-dominant colorectal metastases. *Cardiovasc Intervent Radiol*. 2012;35:1066–73. <https://doi.org/10.1007/s00270-011-0234-7>.
- Cremonesi M, Chiesa C, Strigari L, Ferrari M, Botta F, Guerriero F, et al. Radioembolization of hepatic lesions from a radiobiology and dosimetric perspective. *Front Oncol*. 2014;4:210. <https://doi.org/10.3389/fonc.2014.00210>.
- Garin E, Rolland Y, Laffont S, Edeline J. Clinical impact of (99m)Tc-MAA SPECT/CT-based dosimetry in the radioembolization of liver malignancies with (90)Y-loaded microspheres. *Eur J Nucl Med Mol Imaging*. 2016;43:559–75. <https://doi.org/10.1007/s00259-015-3157-8>.
- Dezarn WA, Cessna JT, DeWerd LA, Feng W, Gates VL, Halama J, et al. Recommendations of the American Association of Physicists in Medicine on dosimetry, imaging, and quality assurance procedures for 90Y microsphere brachytherapy in the treatment of hepatic malignancies. *Med Phys*. 2011;38:4824–45. <https://doi.org/10.1118/1.3608909>.
- Bolch WE, Bouchet LG, Robertson JS, Wessels BW, Siegel JA, Howell RW, et al. MIRD pamphlet No. 17: the dosimetry of non-uniform activity distributions—radionuclide S values at the voxel level. Medical Internal Radiation Dose Committee. *J Nucl Med*. 1999;40:11S–36S.
- Wondergem M, Smits ML, Elschot M, de Jong HW, Verkooijen HM, van den Bosch MA, et al. 99mTc-macroaggregated albumin poorly predicts the intrahepatic distribution of 90Y resin microspheres in hepatic radioembolization. *J Nucl Med*. 2013;54:1294–301. <https://doi.org/10.2967/jnumed.112.117614>.
- Lambert B, Mertens J, Sturm EJ, Stienaers S, Defreyne L, D'Asseler Y. 99mTc-labelled macroaggregated albumin (MAA) scintigraphy for planning treatment with 90Y microspheres. *Eur J Nucl Med Mol Imaging*. 2010;37:2328–33. <https://doi.org/10.1007/s00259-010-1566-2>.
- Ulrich G, Dudeck O, Furth C, Ruf J, Grosser OS, Adolf D, et al. Predictive value of intratumoral 99mTc-macroaggregated albumin uptake in patients with colorectal liver metastases scheduled for radioembolization with 90Y-microspheres. *J Nucl Med*. 2013;54:516–22. <https://doi.org/10.2967/jnumed.112.112508>.
- Hung JC, Redfern MG, Mahoney DW, Thorson LM, Wiseman GA. Evaluation of macroaggregated albumin particle sizes for use in pulmonary shunt patient studies. *J Am Pharm Assoc (Wash)*. 2000;40:46–51. [https://doi.org/10.1016/s1086-5802\(16\)31035-x](https://doi.org/10.1016/s1086-5802(16)31035-x).
- Van de Wiele C, Maes A, Brugman E, D'Asseler Y, De Spiegeleer B, Mees G, et al. SIRT of liver metastases: physiological and pathophysiological considerations. *Eur J Nucl Med Mol Imaging*. 2012;39:1646–55. <https://doi.org/10.1007/s00259-012-2189-6>.
- Ahmadzadehfar H, Duan H, Haug AR, Walrand S, Hoffmann M. The role of SPECT/CT in radioembolization of liver tumours. *Eur J Nucl Med Mol Imaging*. 2014;41(Suppl 1):S115–24. <https://doi.org/10.1007/s00259-013-2675-5>.
- Fabbri C, Sarti G, Cremonesi M, Ferrari M, Di Dia A, Agostini M, et al. Quantitative analysis of 90Y Bremsstrahlung SPECT-CT images for application to 3D patient-specific dosimetry. *Cancer Biother Radiopharm*. 2009;24:145–54. <https://doi.org/10.1089/cbr.2008.0543>.
- Lhommel R, Goffette P, Van den Eynde M, Jamar F, Pauwels S, Bilbao JI, et al. Yttrium-90 TOF PET scan demonstrates high-resolution biodistribution after liver SIRT. *Eur J Nucl Med Mol Imaging*. 2009;36:1696. <https://doi.org/10.1007/s00259-009-1210-1>.
- Padia SA, Alessio A, Kwan SW, Lewis DH, Vaidya S, Minoshima S. Comparison of positron emission tomography and bremsstrahlung imaging to detect particle distribution in patients undergoing yttrium-90 radioembolization for large hepatocellular carcinomas or associated portal vein thrombosis. *J Vasc Interv Radiol*. 2013;24:1147–53. <https://doi.org/10.1016/j.jvir.2013.04.018>.
- Mikell JK, Mahvash A, Siman W, Mourtada F, Kappadath SC. Comparing voxel-based absorbed dosimetry methods in tumors, liver, lung, and at the liver-lung interface for (90)Y microsphere selective internal radiation therapy. *EJNMMI Phys*. 2015;2:16. <https://doi.org/10.1186/s40658-015-0119-y>.
- Chiesa C, Maccauro M, Romito R, Spreafico C, Pellizzari S, Negri A, et al. Need, feasibility and convenience of dosimetric treatment planning in liver selective internal radiation therapy with (90)Y microspheres: the experience of the National Tumor Institute of Milan. *Q J Nucl Med Mol Imaging*. 2011;55:168–97.
- Chiesa C, Mira M, Maccauro M, Spreafico C, Romito R, Morosi C, et al. Radioembolization of hepatocarcinoma with (90)Y glass microspheres: development of an individualized treatment planning strategy based on dosimetry and radiobiology. *Eur J Nucl Med Mol Imaging*. 2015;42:1718–38. <https://doi.org/10.1007/s00259-015-3068-8>.

22. Hsu DFC, Ilan E, Peterson WT, Uribe J, Lubberink M, Levin CS. Studies of a next-generation silicon-photomultiplier-based time-of-flight PET/CT system. *J Nucl Med.* 2017;58:1511–8. <https://doi.org/10.2967/jnumed.117.189514>.
23. Baratto L, Duan H, Ferri V, Khalighi M, Iagaru A. The effect of various beta values on image quality and semiquantitative measurements in 68Ga-RM2 and 68Ga-PSMA-11 PET/MRI images reconstructed with a block sequential regularized expectation maximization algorithm. *Clin Nucl Med.* 2020;45:506–13. <https://doi.org/10.1097/RLU.0000000000003075>.
24. Kao YH, Tan EH, Ng CE, Goh SW. Yttrium-90 time-of-flight PET/CT is superior to Bremsstrahlung SPECT/CT for postradioembolization imaging of microsphere biodistribution. *Clin Nucl Med.* 2011;36:e186–7. <https://doi.org/10.1097/RLU.0b013e31821c9a11>.
25. Kao YH, Tan EH, Lim KY, Ng CE, Goh SW. Yttrium-90 internal pair production imaging using first generation PET/CT provides high-resolution images for qualitative diagnostic purposes. *Br J Radiol.* 2012;85:1018–9. <https://doi.org/10.1259/bjr/33524085>.
26. Elschot M, Vermolen BJ, Lam MG, de Keizer B, van den Bosch MA, de Jong HW. Quantitative comparison of PET and Bremsstrahlung SPECT for imaging the in vivo yttrium-90 microsphere distribution after liver radioembolization. *PLoS One.* 2013;8:e55742. <https://doi.org/10.1371/journal.pone.0055742>.
27. Kunnen B, Beijst C, Lam M, Viergever MA, de Jong H. Comparison of the biograph vision and biograph mCT for quantitative (90)Y PET/CT imaging for radioembolisation. *EJNMMI Phys.* 2020;7:14. <https://doi.org/10.1186/s40658-020-0283-6>.
28. Ilhan H, Goritschan A, Paprottka P, Jakobs TF, Fendler WP, Todica A, et al. Predictive value of 99mTc-MAA SPECT for 90Y-labeled resin microsphere distribution in radioembolization of primary and secondary hepatic tumors. *J Nucl Med.* 2015;56:1654–60. <https://doi.org/10.2967/jnumed.115.162685>.
29. Garin E, Rolland Y, Pracht M, Le Sourd S, Laffont S, Mesbah H, et al. High impact of macroaggregated albumin-based tumour dose on response and overall survival in hepatocellular carcinoma patients treated with (90) Y-loaded glass microsphere radioembolization. *Liver Int.* 2017;37:101–10. <https://doi.org/10.1111/liv.13220>.
30. Ilhan H, Goritschan A, Paprottka P, Jakobs TF, Fendler WP, Bartenstein P, et al. Systematic evaluation of tumoral 99mTc-MAA uptake using SPECT and SPECT/CT in 502 patients before 90Y radioembolization. *J Nucl Med.* 2015;56:333–8. <https://doi.org/10.2967/jnumed.114.150565>.
31. Haste P, Tann M, Persohn S, LaRoche T, Aaron V, Mauxion T, et al. Correlation of technetium-99 m macroaggregated albumin and yttrium-90 glass microsphere biodistribution in hepatocellular carcinoma: a retrospective review of pretreatment single photon emission CT and posttreatment positron emission tomography/CT. *J Vasc Interv Radiol.* 2017;28:722–30 e1. <https://doi.org/10.1016/j.jvir.2016.12.1221>.

**Publisher's note** Springer Nature remains neutral with regard to jurisdictional claims in published maps and institutional affiliations.